

BI-SCALE LMS EQUALIZATION FOR IMPROVED PERFORMANCE

A. A. (Louis) Beex

and

Takeshi Ikuma

DSPRL – Wireless@VT – ECE 0111
Virginia Tech
Blacksburg, VA 24061-0111, USA

Electrical & Computer Engineering
Louisiana State University
Baton Rouge, LA 70806, USA

ABSTRACT

Recent results show that an adaptive transversal least-mean-square (LMS) equalizer in a narrowband-interference dominated environment operates at a mean weight vector that is different from that of the Wiener equalizer of the same structure. In addition, the time-varying component of the LMS weight vector results in a steady-state mean square error (MSE) that can be substantially lower than that for the fixed Wiener equalizer. However, the MSE for this LMS equalizer is higher than the MSE prediction in which LMS is assumed to be operating in a neighborhood of the Wiener weight vector. We find that – although the transversal LMS equalizer itself does not produce the Wiener weight vector as its steady-state mean – the adaptive algorithm can be modified so that its mean weight vector is the fixed Wiener weight vector, while simultaneously facilitating the time-varying weight behavior that is responsible for the reduction in MSE. The resulting bi-scale LMS (BLMS) algorithm achieves further improvement in MSE.

Index Terms— LMS, equalization, nonlinear effects, narrowband interference mitigation, bi-scale LMS

1. INTRODUCTION

In various applications involving narrowband processes, such as noise canceling, prediction, and equalization in interference-dominated environments, transversal least mean square (LMS) adaptive filters will often perform better than expected from the optimal filters of the same structure [1-4]. These non-linear or non-Wiener effects are due to the capability of adaptive filters to produce dynamic, time-varying behavior in their weights [3-5].

It was shown recently that in the adaptive equalization scenario, where the transversal equalizer is used primarily to mitigate narrowband interference, the steady-state mean of the LMS weight vector is different from that of the fixed Wiener equalizer of the same structure. As a result the prediction of mean square error (MSE) performance of such an equalizer [4, 6] needed to be modified, by taking into account the spiral weight mean associated with the LMS algorithm. The resulting MSE prediction was shown to be a

better predictor of MSE performance for the entire range of mean-square stable step-sizes for LMS [7].

We present a new algorithm, derived from LMS, which further improves MSE performance of the adaptive equalizer used for mitigation of narrowband interference.

In Section 2 the MSE performance of the LMS equalizer operating in non-Wiener mode is reviewed, with emphasis on its transient behavior for different weight initializations. We then introduce periodic resetting of the LMS weights to illustrate that the MSE of the equalizer can be improved. The insight gained is used in Section 3 to define the bi-scale LMS algorithm (BLMS). The MSE performance of BLMS is then illustrated and compared to that of the corresponding LMS algorithm.

2. ADAPTIVE EQUALIZATION

In Fig. 1, the setup of the adaptive equalizer for mitigation of narrowband interference is indicated. The adaptive equalizer takes the input signal u_n , which consists of a desired communication signal x_n , additive white complex Gaussian noise n_n , and cisoid interference i_n . Although equalizers are usually employed to mitigate the channel effect on x_n , we assume in this paper that the channel is ideal as we are interested in the equalizer behavior when mitigating narrowband interference. All signals are at complex baseband and sampled at the symbol rate of x_n .

The transversal adaptive equalizer forms an M -tap input vector

$$\mathbf{u}_n = [u_n \quad u_{n-1} \quad \cdots \quad u_{n-M+1}]^T \quad (1)$$

and produces its output

$$y_n = \mathbf{w}_n^H \mathbf{u}_n \quad (2)$$

where $\mathbf{w}_n \triangleq [w_0 \quad w_1 \quad \cdots \quad w_{M-1}]^T$ is the adapted weight vector. Here, $[\]^T$ and $[\]^H$ denote the transpose and conjugate transpose operators, respectively. The LMS algorithm updates \mathbf{w}_n with the “desired” signal d_n by

$$\mathbf{w}_{n+1} = \mathbf{w}_n + \mu \mathbf{u}_n e_n^* \quad (3)$$

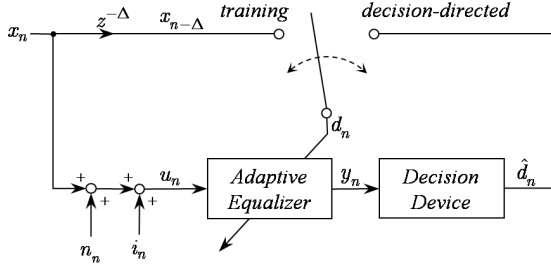


Fig. 1. Simplified adaptive equalizer setup for analysis under narrowband interference conditions.

with the error

$$e_n = d_n - y_n \quad (4)$$

Two possible operating modes of the equalizer alter the source of the desired signal. In training mode, $d_n = x_{n-\Delta}$, a delayed version of the transmitted symbol sequence. In decision-directed mode, $d_n = \hat{d}_n$ where \hat{d}_n is the symbol decision made by the decision device given y_n . In the remainder of this paper, we use $d_n = x_{n-\Delta}$, assuming that the system is running in training mode or in decision-directed mode with very low decision error rate.

For a fixed equalizer, the optimal weight vector \mathbf{w}_w can be found by solving the Wiener-Hopf equation

$$\mathbf{E}[\mathbf{u}_n \mathbf{u}_n^H] \mathbf{w}_w = \mathbf{E}[\mathbf{u}_n d_n^*]. \quad (5)$$

The resulting optimal Wiener filter is [4]

$$\mathbf{w}_w = \eta \left(\mathbf{p}_\Delta - \frac{\sigma_i^2}{\lambda_{\max}} \mathbf{e} \right) \quad (6)$$

and the associated MSE is found to be

$$J_w \triangleq \eta \left(\sigma_n^2 + \sigma_s^2 \frac{\sigma_i^2}{\lambda_{\max}} \right). \quad (7)$$

Here,

$$\mathbf{p}_\Delta \triangleq \underbrace{[0 \ \cdots \ 0]}_{\Delta} \ [1 \ 0 \ \cdots \ 0]^T, \quad (8)$$

$$\mathbf{e} \triangleq e^{j\omega_i \Delta} [1 \ e^{-j\omega_i} \ \cdots \ e^{-j\omega_i(M-1)}]^T, \quad (9)$$

$$\eta \triangleq \frac{\sigma_s^2}{\sigma_s^2 + \sigma_n^2}, \quad (10)$$

and

$$\lambda_{\max} \triangleq \sigma_s^2 + \sigma_n^2 + M\sigma_i^2. \quad (11)$$

with signal power σ_s^2 , noise power σ_n^2 , interference power σ_i^2 , and interference frequency ω_i .

However, when the equalizer is adapted using the LMS algorithm, the elements of the steady-state mean $\bar{\mathbf{w}}_\infty$ of the weights form a spiral for large step-size parameter μ [4]:

$$\bar{\mathbf{w}}_\infty \triangleq \eta (\mathbf{p}_\Delta - \mathbf{v}_\infty) \quad (12)$$

where

$$\bar{\mathbf{v}}_\infty \triangleq \frac{\sigma_i^2}{\lambda_{\max}} (\mathbf{I} - \mu \mathbf{\Xi} \mathbf{\Theta})^{-1} \mathbf{e}, \quad (13)$$

$$\mathbf{\Xi} \triangleq \frac{1}{\sigma_x^2} \left(\mathbf{I} - \frac{\sigma_i^2}{\lambda_{\max}} \mathbf{1} \mathbf{1}^H \right), \quad (14)$$

and

$$\mathbf{\Theta} \triangleq \frac{\sigma_i^2 M}{\sigma_x^2} \sum_{p=1}^{M-1} \mathbf{Z}^p (1 - \mu \lambda_{\max})^{p-1}. \quad (15)$$

In the above, \mathbf{I} is the identity matrix, $\mathbf{1}$ is the vector of all ones, and \mathbf{Z} is the lower triangular shift matrix (ones on the subdiagonal and zeros elsewhere). Furthermore, the steady-state MSE, under large interference-to-signal ratio (ISR), is found to be [4]

$$J_\infty = J(\bar{\mathbf{v}}_\infty) \quad (16)$$

where

$$J(\mathbf{v}) \triangleq \frac{2\eta}{1+\alpha} \left[\sigma_n^2 + \sigma_s^2 |\mathbf{v}|^T \{ \mathbf{I} - (1-\alpha) \mathbf{A} \} |\mathbf{v}| \right], \quad (17)$$

$$\mathbf{A} \triangleq \begin{bmatrix} 0 & \cdots & 0 \\ 1 & 0 & & \\ \alpha & 1 & \ddots & \vdots \\ \vdots & & & 0 \\ \alpha^{M-2} & \cdots & \alpha & 1 & 0 \end{bmatrix}, \quad (18)$$

and

$$\alpha \triangleq 1 - \mu \sigma_i^2 M. \quad (19)$$

2.1. Transient MSE characteristics

The transient behavior of the LMS equalizer with large step-size parameter is studied via numerical simulation in the remainder of this section. The scenario we use for illustration uses an adaptive transversal equalizer ($M = 7$) with step-size $\mu = \lambda_{\max}^{-1}$ with 25-dB SNR and 20-dB ISR. The fractional interference frequency used throughout is $\omega_i = 2\pi(0.1)$. A QPSK signal with random symbols is used as x_n . The estimated MSE is denoted as \hat{J}_n .

The transient MSE performance of this equalizer is illustrated in Fig. 2, for having initialized with the weight vector set to the all-zero vector ($\mathbf{w}_0 = \mathbf{0}$) and set to the Wiener weight vector ($\mathbf{w}_0 = \mathbf{w}_w$), respectively. Unless

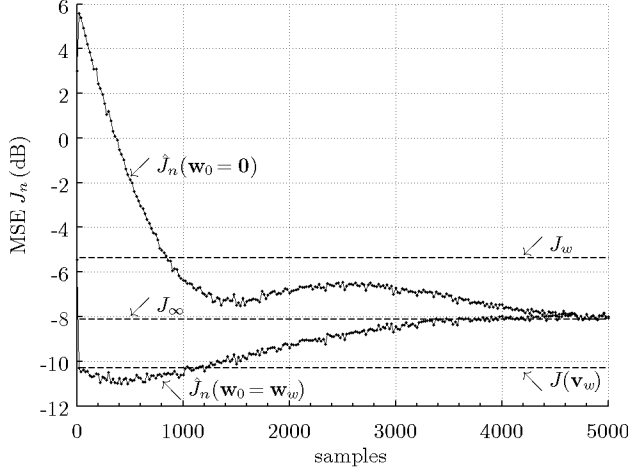


Fig. 2. MSE performance of the LMS equalizer in transient (data plotted every 20 iterations).

noted otherwise, all figures below show averages based on 1000 independent runs. Note that – for each of these initializations – the LMS equalizer converges to the theoretical steady-state MSE performance J_∞ which is below J_w , the MSE of the (fixed) Wiener equalizer; this phenomenon is due to the non-Wiener effect. Lastly, $J(\mathbf{v}_w)$ represents the MSE expression in (17) evaluated with the Wiener weights, for which $\mathbf{v}_w = \mathbf{p}_\Delta - \eta^{-1} \mathbf{w}_w$ (from (6) and (12)).

The most remarkable observation here is that when the LMS equalizer is started from \mathbf{w}_w $\hat{J}_n < J_\infty$ is realized during the transient; in fact, the steady-state MSE is being approached from below. Also, at the beginning of the transient – i.e., when $\mathbf{w}_n \approx \mathbf{w}_w$ – we get $\hat{J}_n \approx J(\mathbf{v}_w)$ when the LMS equalizer is started from \mathbf{w}_w . The latter observation leads to Fig. 3 in which the transient MSE is semi-analytically derived from (17) and the experimental ensemble average $\hat{\mathbf{w}}_n$ of the LMS weight vector. Here, (17) is evaluated with $\hat{\mathbf{v}}_n = \mathbf{p}_\Delta - \eta^{-1} \hat{\mathbf{w}}_n$. The plot includes a third simulation result with the weight vector initialized to $\bar{\mathbf{w}}_\infty$, illustrating that the LMS equalizer then operates in steady state immediately.

The agreement shown in Fig. 3 between \hat{J}_n and $J(\hat{\mathbf{v}}_n)$ for the various initialization cases suggests that (17) provides a very good indication of not only the steady-state MSE, but also of the transient MSE characteristics of the LMS equalizer given its average LMS weight behavior. We also note that the observed convergence of $J(\hat{\mathbf{v}}_n)$ to J_∞ is supported by the convergence of $\hat{\mathbf{w}}_n$ to $\bar{\mathbf{w}}_\infty$.

2.2. Periodic resetting of weights

From Fig. 2 and Fig. 3, it is clear that the Wiener weight is not a stationary point for the LMS equalizer. However, when started off at the Wiener weight, the LMS equalizer lingers at an MSE lower than the predicted steady-state

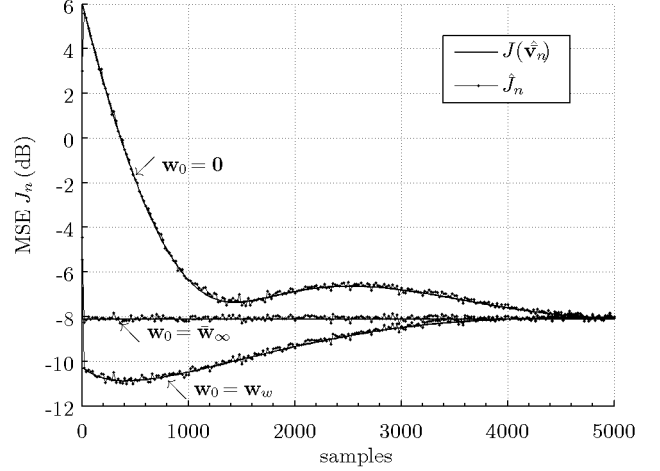


Fig. 3. Semi-analytical transient MSE model.

MSE value it converges to later. Specifically, during the first 1,000 iterations, the transient MSE is 2 dB (or more) lower than the steady-state MSE.

The observed behavior suggests that the LMS equalizer can attain a better “steady-state” MSE by periodically resetting the adaptive weights to the Wiener weights; in other words, forcing the adaptation to be permanently in a transient mode. The weight reset,

$$\mathbf{w}_n = \mathbf{w}_w, \quad (20)$$

is performed when $n = kN_r$ with $k \in \mathbb{Z}$ and the reset period N_r . The reset operation occurs after (2) and before (3) during the LMS filtering process. In addition to the weight reset, the error is computed based on the Wiener weights, i.e.

$$e_n^{(\text{reset})} = d_n - \mathbf{w}_w^H \mathbf{u}_n \quad (21)$$

Combining (3), (20), and (21), the weight update with reset step can be seen to be

$$\mathbf{w}_{n+1} = (\mathbf{I} - \mu \mathbf{u}_n \mathbf{u}_n^H) \mathbf{w}_w + \mu \mathbf{u}_n d_n^*. \quad (22)$$

The result of such resetting with $N_r = 1000$ iterations is demonstrated in Fig. 4. The squared norm of the mean weight vector is included to illustrate the weight resetting operation. We observe that the resetting operation realizes the anticipated equalizer MSE performance.

Of course, having to use a priori information for resetting – such as the Wiener weight – defeats the purpose of using an adaptive algorithm. In the next section, we move towards a fully adaptive algorithm, in which no periodic resetting is used.

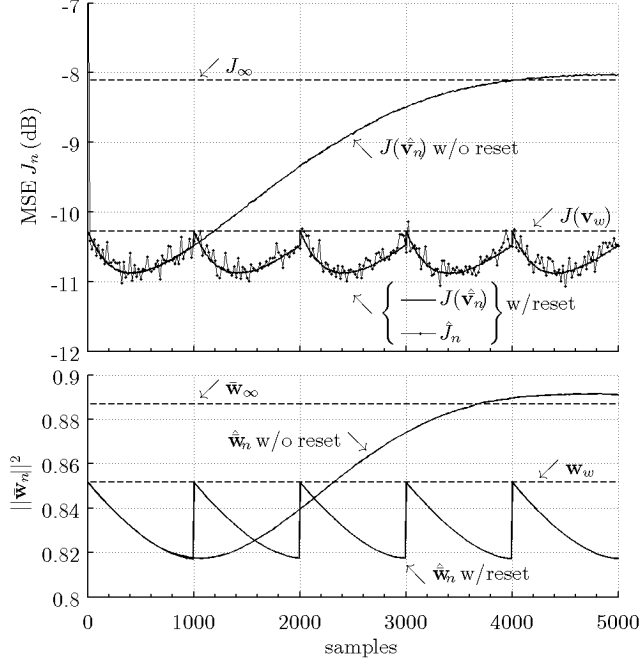


Fig. 4. MSE performance with periodic reset to \mathbf{w}_w ($N_r = 1000$) (top) and mean squared norm of weight vector (bottom).

3. BI-SCALE LMS EQUALIZER

As a result of the observations in the previous section, we hypothesize that consistently low MSE can be produced by an adaptive algorithm that exhibits behavior characteristics associated with two adaptation time scales. On the one hand, it maintains a mean weight vector in the neighborhood of the (fixed) Wiener equalizer – as results from slow time-scale LMS adaptation – while on the other hand allowing time-varying weight behavior similar to that in large step-size LMS, i.e. fast time-scale adaptation. This leads us to propose the bi-scale LMS algorithm (BLMS) with two sets of weights, $\{\mathbf{w}_{S,n}, \mathbf{w}_{L,n}\}$.

$$\tilde{y}_n = \mathbf{w}_{L,n}^H \mathbf{u}_n \quad (23)$$

$$\varepsilon_n = d_n - \mathbf{w}_{S,n}^H \mathbf{u}_n \quad (24)$$

$$\mathbf{w}_{S,n+1} = \mathbf{w}_{S,n} + \mu_S \mathbf{u}_n \varepsilon_n^* \quad (25)$$

$$\mathbf{w}_{L,n+1} = \mathbf{w}_{L,n} + \mu_L \mathbf{u}_n \varepsilon_n^* \quad (26)$$

Note that (24) and (25) constitute the usual LMS algorithm. The step-size subscript S indicates that the step-size used is small, so that the weight vector in (25) tends to the optimal (fixed) Wiener weight vector as step-size is smaller and smaller. We note that the error process ε_n , as computed in (24), is the small step-size LMS error signal. As a result of the small step-size, any time-varying weight behavior tends

to be suppressed in $\mathbf{w}_{S,n}$. The bi-scale LMS algorithm component in (26) uses the conventional LMS weight update equation but with the error of the small step-size LMS together with a large step-size μ_L to produce a correction to the small step-size weight vector $\mathbf{w}_{S,n}$. The large step-size tends to maintain the instantaneous time-varying behavior of the non-Wiener weight behavior and its associated beneficial effects. The performance of BLMS is measured by its a priori error,

$$\tilde{e}_n = d_n - \tilde{y}_n, \quad (27)$$

and the MSE derived from it is denoted as $J_{B,n} \triangleq E[|\tilde{e}_n|^2]$. As indicated by Fig. 4 (the bottom plot), even though a large step-size is used, the LMS weights adapt very slowly under the large ISR scenario, due to the large eigenvalue spread of the input correlation matrix. Hence, $\mathbf{w}_{L,n+1}$ is an instantaneously perturbed version of $\mathbf{w}_{S,n}$, and we can assume (and have verified) that $\bar{\mathbf{w}}_L \approx \bar{\mathbf{w}}_S$. Moreover, when a small enough step-size μ_S is used the result is that $\bar{\mathbf{w}}_S \approx \mathbf{w}_w$ in steady state. Hence, the steady-state MSE $J_{B,\infty}$ is predicted well by $J(\mathbf{v}_w)$ when $\mu_L = \lambda_{\max}^{-1}$ and provides a good indication of the beneficial performance due to non-Wiener weight behavior.

3.1. Steady-state performance of the BLMS equalizer

The steady-state MSE performance of the BLMS equalizer is evaluated numerically in this section. The simulation signal configurations from Section 2 are used again; i.e., QPSK signal at 20-dB ISR, 25-dB SNR, and interference frequency $2\pi(0.1)$.

First, Fig. 5 shows the steady-state MSE performance of the equalizers as a function of the number of taps of the LMS and BLMS filters. The LMS algorithm uses $\mu = \lambda_{\max}^{-1}$ while the BLMS algorithm uses $\mu_S = 0.001\lambda_{\max}^{-1}$ and $\mu_L = \lambda_{\max}^{-1}$. Both equalizers use $\Delta = 0$. The steady-state MSE estimates obtained via time-averaging 10000 steady-state error samples in simulation are denoted as $\hat{J}_{B,\infty}$ for the BLMS algorithm and \hat{J}_∞ for the LMS algorithm.

The MSE estimates obtained from simulations agree very well with the analytical MSEs, i.e., $J(\bar{\mathbf{v}}_\infty)$ for the LMS equalizer and $J(\mathbf{v}_w)$ for the BLMS equalizer. The BLMS equalizer performs better than the LMS equalizer, and both are superior to the fixed Wiener equalizer with the same transversal structure.

Next, in Fig. 6, the steady-state MSE performance of the two equalizers is assessed as the step-size parameters are varied. The step-size μ_L for the BLMS algorithm is varied, while the step-size μ of the LMS algorithm is kept equal to it. The step-size μ_S in BLMS is fixed to $\mu_S = 0.001\mu_L$ for all cases. Both algorithms use $M = 7$ in this experiment.

What is observed in Fig. 6 is intriguing. As expected from Fig. 5, the observed BLMS MSE curve $\hat{J}_{B,\infty}$ matches $J(\mathbf{v}_w)$ at $\mu_L = \lambda_{\max}^{-1}$. However, for all other values of μ_L

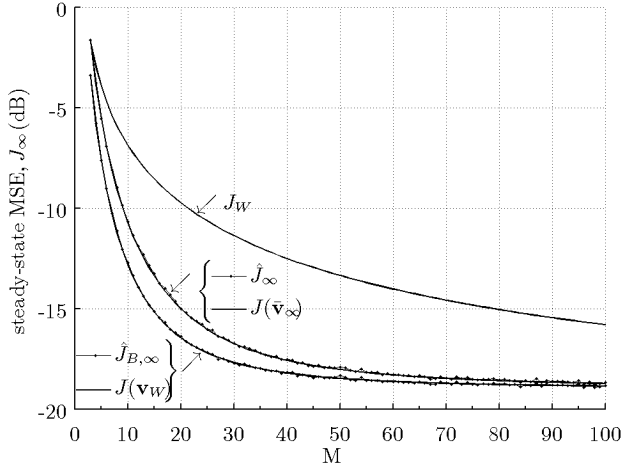


Fig. 5. Steady-state MSE performance of LMS and BLMS equalizers vs. number of taps.

(except for zero) the BLMS performance curve $\hat{J}_{B,\infty}$ no longer agrees with the $J(\mathbf{v}_w)$ curve. Moreover, at $\mu_L \approx 0.8\lambda_{\max}^{-1}$, the BLMS equalizer attains even lower MSE than that predicted by $J(\mathbf{v}_w)$. We are investigating the causes of the latter phenomenon, as well as its potential for further improvement of the algorithm.

4. CONCLUSIONS

We have shown that the predicted MSE performance of an adaptive equalizer for narrowband interference mitigation, based on a mean weight vector equal to the mean Wiener weight vector, can be very well approached by modifying the LMS algorithm so that it has the assumed properties. This modification resulted in the proposed bi-scale LMS, which simultaneously uses two very different time scales of adaptation; a very slow time scale to approach the mean Wiener weight as its steady state mean weight vector and a very fast time scale to generate the time-varying, dynamic weight behavior that was shown to lead to performance improvement. The design of a better algorithm appears to be a possibility, as – for some step-sizes – the current approach produces even better MSE performance than predicted on the basis of the Wiener weight vector as the steady-state mean weight.

5. REFERENCES

[1] R. C. North, R. A. Axford, and J. R. Zeidler, "The performance of adaptive equalization for digital communication systems

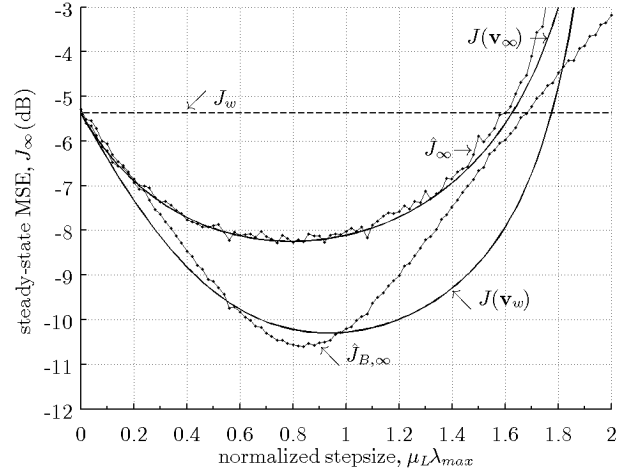


Fig. 6. Steady-state MSE performance of BLMS and LMS equalizers vs. step-size.

corrupted by interference," in *27th Asilomar Conf.*, Pacific Grove, CA, 1993, pp. 1548-1553.

- [2] M. Reuter and J. R. Zeidler, "Nonlinear effects in LMS adaptive equalizers," *IEEE Transactions on Signal Processing*, vol. 47, pp. 1570-1579, June 1999.
- [3] A. A. Beex and J. R. Zeidler, "Steady-state dynamic weight behavior in (N)LMS adaptive filters," in *Least-Mean-Square Adaptive Filters*, S. Haykin and B. Widrow, Eds. Hoboken, NJ: John Wiley & Sons, 2003, pp. 335-443.
- [4] T. Ikuma, "Non-Wiener effects in narrowband interference mitigation using adaptive transversal equalizers," Ph.D. Dissertation, Dept. Elect. Comput. Eng., Virginia Tech, Blacksburg, 2007. [Online]. Available: <http://scholar.lib.vt.edu/theses/available/etd-04112007-104316/>
- [5] A. A. Beex and T. Ikuma, "Nonlinear dynamic effects of adaptive filtering in narrowband interference-dominated environments," in *ICAND'07*, Kauai, Hawaii, 2007.
- [6] T. Ikuma, A. A. Beex, and J. R. Zeidler, "Non-Wiener weight behavior of LMS transversal equalizers," in *Proc. 32nd IEEE Int. Conf. Acoustics, Speech, Signal Processing*, Honolulu, HI, 2007, pp. 1297-1300.
- [7] T. Ikuma and A. A. Beex, "Improved mean square error estimate for the LMS transversal equalizer with narrowband interference," *IEEE Transactions on Signal Processing*, Accepted.